High permeation rates in liposome systems explain rapid glyphosate biodegradation associated with strong isotope fractionation

Benno N. Ehrl,[†] Emmanuel O. Mogusu,[†,¶] Kyoungtea Kim,[‡] Heike Hofstetter,[§] Joel Pedersen,[,‡,§,∥] Martin Elsner[*,†,□]*

[†] Institute of Groundwater Ecology, Helmholtz Zentrum München, Ingolstädter Landstrasse 1, 85764 Neuherberg, Germany

[¶] Department of Chemistry, Mwenge Catholic University, P.O.BOX 1226, Moshi, Tanzania

[‡] Molecular and Environmental Toxicology Center, University of Wisconsin, Madison, WI 53706, USA

[§] Department of Chemistry, University of Wisconsin, Madison, WI 53706, USA

[‡] Departments of Soil Science and Civil & Environmental Chemistry, University of Wisconsin, Madison, WI 53706, USA

[□] Institute of Hydrochemistry, Chair for Analytical Chemistry and Water Chemistry, Technical University of Munich, Marchioninistrasse 17, 81377 Munich, Germany

Published as "Ehrl, B., Mogusu, E.O., Kim, K., Hofstetter, H., Pedersen, J.A., Elsner, M.: High permeation rates in liposome systems explain rapid glyphosate biodegradation associated with strong isotope fractionation. Environ. Sci. Technol. 52, 7259-7268 (2018), doi: 10.1021/acs.est.8b01004"

Abstract: Bacterial uptake of charged organic pollutants such as the widely used herbicide glyphosate is typically attributed to active transporters, whereas passive membrane permeation as an uptake pathway is usually neglected. For 1-palmitoyl-2-oleoyl-*sn*-glycero-3-phosphocholine (POPC) liposomes, the pH-dependent membrane permeation coefficients (P_{app}) of glyphosate, determined by nuclear magnetic resonance (NMR) spectroscopy, varied from P_{app}(pH 7.0) = 3.7 (± 0.3) × 10^{-7} m·s^{-1} to P_{app}(pH 4.1) = 4.2 (± 0.1) × 10^{-6} m·s^{-1}. The magnitude of this surprisingly rapid membrane permeation depended on glyphosate speciation and was, at physiological pH, in the range of polar, non-charged molecules. These findings point to passive membrane permeation as potential uptake pathway during glyphosate biodegradation. To test this hypothesis, a Gram-negative glyphosate degrader, *Ochrobactrum sp.* FrEM, was isolated from glyphosate-treated soil and glyphosate permeation rates inferred from the liposome model system were compared to bacterial degradation rates. Estimated maximum permeation rates were, indeed, two orders of magnitudes higher than degradation rates of glyphosate. In addition, biodegradation of millimolar glyphosate concentrations gave rise to pronounced carbon isotope fractionation with an apparent kinetic isotope effect, $AKIE_{carbon}$= 1.014 ± 0.003. This value lies in the range typical of unmasked enzymatic isotope fractionation demonstrating that glyphosate biodegradation was little mass transfer-limited and glyphosate exchange across the cell membrane was rapid relative to enzymatic turnover.

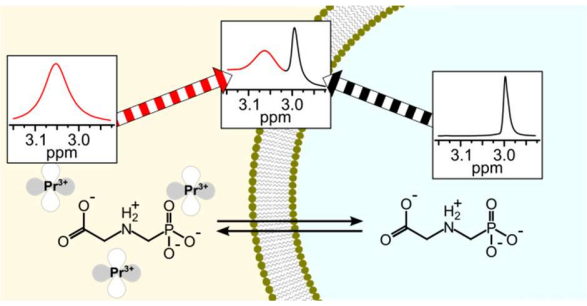

Abstract art

INTRODUCTION

Glyphosate (*N*-(phopshomethyl)glycine) is a systemic, post-emergent, non-selective herbicide widely used in agriculture because of its ability to effectively control a broad range of weeds.[1-3] One component of its success has been the introduction of transgenic, glyphosate-resistant crops.[4, 5] The worldwide market share of glyphosate is estimated at USD 5.6 billion, with the USGS estimating glyphosate use at more than 130,000 tons in 2015 alone in the USA.[2, 6, 7] Historically, the acute toxicity of glyphosate was considered to be low;[3] it appears, however, that the impact of glyphosate on the environment has been underestimated:[8-10] Most importantly, the ubiquitous use of glyphosate has been found to affect biodiversity,[11] which is aggravated by increased usage due to the planting of glyphosate-resistant crops.[12, 13] The effect of glyphosate on human health is currently disputed. After the World Health Organization classified glyphosate as "probably carcinogenic" to humans (Group 2A),[14] discussion has continued on whether or not glyphosate use poses a cancer risk.[15, 16,] In addition, the detection of glyphosate and its metabolite aminomethylphosphonic acid (AMPA) in surface waters and groundwaters at increasing frequencies lends urgency to the need to more thoroughly explore its environmental fate.[17-19] In particular, an improved understanding is warranted on the key drivers that limit its natural microbial degradation, because biodegradation represents the most effective glyphosate remediation pathway.[20-23]

Recent work highlights the particular role of pollutant mass transfer into microbial cells as a rate-limiting step for biodegradation, especially at low pollutant concentrations.[24, 25] The mass transfer of polar and charged species (e.g., zwitterionic glyphosate[26]) into bacterial cells is currently assumed to occur by active transport.[27, 28] Little is known whether charged molecules can directly permeate the cell membrane as non-polar pollutants do,[29, 30] and if so, to what extent the

62 bacterial membrane as diffusion barrier constitutes an even stronger bioavailability limitation for
63 these charged molecules than for non-charged pollutants.[31] Thus, it is important not only to
64 investigate the membrane permeation rate but also to identify whether the rate of glyphosate is
65 determined by the enzymatic reaction or by slow mass transfer of the herbicide across the cell
66 envelope[28, 32] (where mass transfer can occur by either membrane permeation[31] or active
67 transport[33]).

68 To investigate membrane permeation processes, different model systems, ranging from the *n*-
69 octanol-water distribution coefficient as a surrogate to partitioning to membrane lipids to more
70 complex systems like lipid discs and black lipid membranes, to synthetic membranes[34, 35] are used
71 to study the diffusion of drugs and cosmetics through human epithelia.[36-38] However, these model
72 systems typically contain non-natural lipid phases or non-natural lipid-water interfaces. Therefore,
73 membranes resembling biological lipid bilayers (e.g., liposomes with natural lipid composition)
74 are currently the best model to approximate permeation rates valid for natural systems.[39, 40] Here,
75 we used unilamellar liposomes composed of a single zwitterionic phospholipid, 1-palmitoyl-2-
76 oleoyl-*sn*-glycero-3-phosphocholine (POPC), as a simplified system to investigate the permeation
77 of glyphosate across phospholipid bilayers.[41] The POPC vesicles have a gel-to-liquid crystalline
78 phase transition temperature of –2 °C and under our experimental condition are in the liquid
79 crystalline phase, resembling the dominant state of membranes of many bacteria.[42, 43] This model
80 system lacked additional membrane constituents (e.g., anionic lipids, proteins,
81 lipopolysaccharides) and cell envelope structures (phase-segregated domains in membranes,
82 double membrane in Gram-negative bacteria, peptidoglycan cell wall) that are present in bacterial
83 cells.[44] We note that porins in the Gram-negative bacterial outer membrane permit passage of

84 hydrophilic molecules with molecular masses $\lesssim$ 600 Da[29] and the large pores of peptidoglycan do
85 not restrict pollutant permeation.[45]

86 Permeation of the phospholipid bilayer leads to chemical exchange between the outside and the
87 inside of the liposomes. Nuclear magnetic resonance (NMR) spectroscopy offers a direct approach
88 to quantify the permeation process based on the following principle. A nucleus gives rise to an
89 NMR signal at a chemical shift that reflects its chemical environment. Liposomes prepared and
90 suspended in the same solution have roughly equivalent chemical environments inside and outside
91 the liposome. Addition of a non-permeable chemical shift agent (such as a lanthanide ion) to the
92 solution either interior or exterior to the liposome alters the chemical environments on the inside
93 vis-à-vis the outside of the liposome (as the shift agent cannot cross the lipid bilayer) and results
94 in distinct peaks in the NMR spectrum for the nucleus inside and outside the lipososmes.[37, 41, 46]
95 (In the present study, praseodymium (III) ions (Pr^{3+}) were added to the solution external to the
96 liposomes as a non-permeating chemical shift agent.) When the apparent exchange rate constant
97 (k_{tr}) between the two chemical environments (here, inside and outside the liposomes) is smaller
98 than the observed frequency difference between the two states ($\Delta\upsilon$), dynamic exchange of nuclei
99 between chemical environments at equilibrium leads to line broadening.[47] Lineshape analysis
100 subsequently allows quantification of chemical exchange of between both environments based on
101 the evaluation of associated line broadening in the NMR spectrum.[47]

102 Complementary to these model systems, we recently advanced compound-specific isotope
103 analysis (CSIA) as an analytical approach to trace limitations of mass transfer across the cell
104 envelope directly *in vivo* while pollutant biodegradation is ongoing.[25, 31] The underlying principle
105 is the kinetic isotope effect of the associated enzymatic reaction. As the activation energy during
106 a biochemical reaction is higher for bonds containing a heavy isotope, the turnover of molecules

107 with a heavy isotope in the reactive position is slower. Therefore, as the enzymatic reaction
108 proceeds, molecules containing heavy isotopes become enriched in the residual (non-reacted)
109 substrate relative to those with light isotopes.[48] This trend can be evaluated by relating the change
110 in isotope ratio (R_t/R_o) to the fraction of the remaining pollutant f according to the Rayleigh
111 equation[49, 50] (1)

$$\ln\left(\frac{R_t}{R_0}\right) = \ln\left(\frac{\delta^{13}C_t + 1}{\delta^{13}C_0 + 1}\right) = \varepsilon \times ln(f) \quad (1)$$

112 where the enrichment factor ε describes how much slower heavy isotopes react compared to
113 light isotopes. Here, the carbon isotope values $\delta^{13}C_t$ and $\delta^{13}C_0$ at time t and at the beginning of a
114 reaction, respectively, are expressed relative to an international reference material $\delta^{13}C = (R_{\text{Sample}}$
115 $- R_{\text{Reference}})/ R_{\text{Reference}}$ to ensure comparability between laboratories. Thullner *et al.* delineated a new
116 angle to use the change in isotope ratio as a diagnostic tool to directly observe mass-transfer
117 limitation: strong isotope fractionation is observable, only if the pollutant exchange across the cell
118 envelope is faster than its enzymatic turnover. Otherwise substrate molecules which experience
119 the isotopic discrimination during the enzymatic reaction in the cytosol are used up completely so
120 that they do not return to the bulk solution where the isotope ratio is assessed.[51-53] As a
121 consequence, the enzymatic isotope fractionation that is observable in solution becomes masked
122 in the presence of mass transfer limitations – i.e., when active transport (or passive membrane
123 permeation) into and out of the cell is the rate-determining step in biodegradation.[25, 33]

124 For this study, we used a combined approach to gain insight into the role of passive permeation
125 for biodegradation of the zwitterionic pollutant glyphosate, which carries either one (pH < 6) or
126 two (pH > 6) net negative charges at circumneutral pH. First, an NMR study was conducted to
127 experimentally determine pH-dependent passive membrane permeation of glyphosate in
128 phosphatidylcholine liposomes as model system. Second, passive permeation rates were

129 extrapolated and compared to biodegradation rates of different glyphosate degraders to elucidate
130 the role of passive membrane permeation of glyphosate for nutrient uptake. To this end,
131 *Ochrobactrum sp.* FrEM, a new glyphosate degrader, was isolated from a vineyard soil treated
132 with glyphosate, characterized, and used for degradation experiments. The isotope fractionation
133 measured during glyphosate biodegradation by *Ochrobactrum sp.* FrEM was explored as a
134 diagnostic tool to directly observe the presence or absence of mass transfer limitations and, thus,
135 to validate the assessment based on the results of the liposome model system and our theoretical
136 considerations.

137 EXPERIMENTAL SECTION

138 **Chemicals.** A list of chemicals used can be found in the Supporting Information (SI).

139 **Liposome preparation and characterization.** A 25 mg·mL^{-1} solution of 1-palmitoyl-2-oleoyl-
140 *sn*-glycero-3-phosphocholine (POPC, transition temperature –2 °C) in chloroform was prepared,
141 and 50 mg POPC (2 mL of the POPC solution) was added to a 3 mL screw cap glass vial tested
142 prior to the experiment to withstand exposure to liquid nitrogen (see below). The chloroform was
143 evaporated under a N_2 stream, and the lipid film was dried with vacuum for at least 12 h. The dried
144 lipids were hydrated with 1 mL of 20 mM glyphosate in D_2O containing a small amount of 3-
145 (trimethylsilyl)-2,2,3,3-tetradeuteropropionic acid (TSP) as internal reference for NMR. The pH
146 of the solution, ranging from pH 4.1 to pH 7.8, was adjusted prior to hydration with 1 M sodium
147 hydroxide (in D_2O). (Effective solvent suppression (*vide infra*) resulted insignificant increase in
148 the HOD peak due to NaOH addition.) The vial was vortexed thoroughly, liposomes formed, and
149 the suspension was subjected to three freeze-thaw cycles (freeze in liquid nitrogen for 5 min, thaw
150 in 40 °C water bath for 5 min, and vortex for 30 s) followed by extrusion to yield unilamellar
151 liposomes of uniform size distribution.[54, 55] The liposomes were extruded in 1000 µL syringes with

152 11 passages through a 0.2 µm polycarbonate filter with an Avanti Mini-Extruder (Avanti Polar
153 Lipids, Inc., USA). The hydrodynamic size and the zeta potential of the vesicles were determined
154 by dynamic light scattering and laser Doppler electrophoresis with a ZetaSizer Nano ZS (Malvern
155 Instruments Ltd., United Kingdom) in dilutions of 2 µL liposome solution in 800 µL D_2O. The
156 temperature of the measurement cell was 25 °C. Ten measurements were averaged for each
157 technical replicate (six replicates for dynamic light scattering and five replicates for laser Doppler
158 electrophoresis).

159 **Nuclear magnetic resonance spectroscopy.** All measurements were carried out on an Avance
160 III 500 MHz spectrometer equipped with a BBFO+ smartprobe (Bruker, USA) at a sample
161 temperature of 25 °C. NMR spectra were recorded with TopSpin 3.5.6 (Bruker, USA).
162 Apodization, Fourier transformation, phase and baseline corrections, absolute referencing on TSP,
163 spectra analysis, and peak fitting was carried out with MestReNova 11.0.3 (Mestrelab Research,
164 Spain). Standard Bruker pulse sequences were used and the spectra collection parameters are
165 summarized in **SI Table S1**.

166 **Assessing the line broadening due to chemical exchange across the liposome membrane.**
167 First, a standard ^{1}H spectrum of 550 µL glyphosate liposome solution was collected to assess the
168 pH-dependent chemical shift of the HOD peak and the chemical shift of the phosphorus nucleus
169 was determined by $^{31}P\{^{1}H\}$. Then, a proton spectrum with phosphorus decoupling $^{1}H\{^{31}P\}$ and
170 solvent suppression was recorded. We added 5.5 µL of a 50 mM $PrCl_3$ solution in D_2O to the NMR
171 tube up to a final concentration of 0.5 mM $PrCl_3$. Another $^{1}H\{^{31}P\}$ spectrum with solvent
172 suppression was recorded and the glyphosate peaks prior to and after $PrCl_3$ addition were
173 compared by fitting of the peaks. The strong $^{2}J_{HP}$ coupling of 12.4 Hz between the phosphorus and
174 adjacent protons led to splitting of the peak at 2.99 ppm into a doublet in the ^{1}H NMR spectrum

175 (**Figure 1**). This doublet, however, complicated peak shape analysis to quantify the rate of
176 glyphosate permeation across liposomes. In the absence of Pr^{3+}, the shape of the separated doublet
177 peaks could be fit. However, addition of Pr^{3+} led to line broadening due to chemical exchange
178 between the inside and the outside of the liposomes. Thus, the individual peaks of the doublet
179 signal overlapped with each other, rendering peak shape analysis unreliable. We therefore used a
180 ^{1}H-NMR pulse sequence that combined solvent suppression (watergate W5) with phosphorus
181 decoupling. As a result, the doublet peak collapsed to a well-resolved singlet that was
182 distinguishable from the POPC liposome signals (**Figure 2A**).

183 **Bacterial isolation and characterization.** For bacterial isolation from soil, mineral salt medium
184 at pH 7.0 containing 60 mM sodium glutamate as carbon source and 38 mM ammonium chloride
185 as nitrogen source. Glyphosate (3 mM) was the sole phosphorous source. A detailed description
186 of the bacterial isolation from vineyard soil can be found in the SI.

187 **Biodegradation of glyphosate by *Ochrobactrum sp.* FrEM**. The biodegradation of glyphosate
188 by *Ochrobactrum sp.* FrEM was carried out in two biological replicates. We inoculated 50 mL of
189 medium (see SI) with *O. sp.* FrEM and incubated the culture at 30 °C at 160 rpm overnight. Cells
190 were harvested by centrifugation (2100 *g*, Heraeus Megafuge 1.0R, Germany), washed twice with
191 medium, and transferred to 50 mL fresh medium lacking phosphorus for phosphorus depletion.
192 After incubation at 30 °C for 48 h, cells were harvested by centrifugation (2100 *g*, Heraeus
193 Megafuge 1.0R, Germany) and used to inoculate 150 mL of medium containing 120 µM
194 glyphosate as the only phosphorus source. Bacterial growth was monitored at OD_{600} with a Cary
195 50 Bio UV-Vis spectrometer (Varian Medical Systems, Inc., USA). During the biodegradation,
196 samples for isotope analysis (10 mL) were taken and the reaction was stopped by adding 1 mL of
197 2 M sodium hydroxide. The samples were lyophilized and reconstituted in water. The water

198 volume for reconstitution was decreased from 5 mL to 2 mL as glyphosate was consumed for
199 glyphosate preconcentration to be within the working range of the isotope measurements (see
200 below). The isotope ratio in the delta notation ($\delta^{13}C$ in per mil relative to Vienna PeeDee Belemnite
201 (V-PDB)) and the concentration of glyphosate were determined by liquid chromatography Isolink-
202 isotope ratio mass spectrometry (LC-IRMS) (Thermo Fisher, Germany). The method used for
203 carbon isotope analysis of glyphosate was modified from Kujawinski *et al.*[56] as follows: A mixed-
204 phase Primesep 100 column 100 x 5.6 mm, 3 µm particle size (SIELC Technologies, USA) was
205 used as stationary phase and 2.5 mM phosphate buffer at pH 3.1 was used as mobile phase.
206 Separation was achieved with 300 $\mu L \cdot min^{-1}$ isocratic flow. The injection volume was 25 µL. The
207 reagents for the chemical conversion to CO_2 at 99.9 °C were 1.5 M phosphoric acid and 0.84 M
208 peroxodisulfate at a flow rate of 50 $\mu L \cdot min^{-1}$ each. The helium (grade 5.0) flow rate in the
209 separation unit was set to 2.3 $mL \cdot min^{-1}$. The glyphosate concentration was determined with the
210 area of the glyphosate CO_2 peak in the LC Isolink-IRMS chromatogram via external calibration
211 with glyphosate standards in water (0.03, 0.06, 0.12, and 0.30 mM).
212
213 **RESULTS AND DISCUSSION**
214 **Praseodymium(III) ions interact with glyphosate as well as the liposome surface.** The
215 liposome preparations were of a uniform size with a hydrodynamic diameter of 204 ± 5 nm
216 (median ± standard deviation) ranging from 194 nm to 239 nm. The median polydispersity index
217 was 0.093 indicating a uniform and narrow size distribution of the individual liposome
218 preparations. The neutral zeta potential of the liposomes composed of lipids bearing zwitterionic
219 phosphatidylcholine headgroups[57] changed to +29 ± 6 mV upon $PrCl_3$ addition, because the
220 strongly positively charged Pr^{3+} associated with the negatively charged phosphate group of POPC.

221 Praseodymium(III) was added to produce a chemical environment outside the liposomes differing
222 from that inside to allow glyphosate exchange across the membrane to be quantified. Indeed,
223 addition of Pr^{3+} resulted in an interaction of glyphosate with the chemical shift agent which led to
224 a position-specific downfield shift $\Delta\delta_H$ of the glyphosate ^{1}H-NMR signals: The chemical shift
225 change produced by a 1 mM $PrCl_3$ solution was $\Delta\delta_H = 0.06$ ppm for the PO_3^{2-}-CH_2-NH_2^+-$C\underline{H_2}$-
226 COO^- protons and $\Delta\delta_H = 0.16$ ppm for the PO_3^{2-}-$C\underline{H_2}$-NH_2^+-CH_2-COO^- protons in the ^{1}H-NMR
227 spectrum of glyphosate (**SI Figure S1**). The phosphorus peak was shifted downfield by
228 $\Delta\delta_P = 1.29$ ppm in the ^{31}P{1H} spectrum (**SI Figure S1**). That the chemical shift change was
229 strongest for the phosphorus peak and weakest for the protons adjacent to the carboxyl group
230 indicated that Pr^{3+} directly interacted with the negatively charged phosphate group and not with
231 the negatively charged carboxyl group of the zwitterionic glyphosate.

232 **The addition of praseodymium(III) and subsequent peak shape analysis quantified**
233 **chemical exchange of glyphosate.** Subsequent addition of 0.5 mM Pr^{3+} to a glyphosate solution
234 without liposomes moved the chemical shift of the collapsed singlet of the PO_3^{2-}–$C\underline{H_2}$–NH_2^+–
235 CH_2-COO^- protons downfield from 2.99 ppm to 3.06 ppm. Interaction with the paramagnetic Pr^{3+}
236 changes in the local magnetic field, leading to the shift in frequency; the association/dissociation
237 of Pr^{3+} and glyphosate produced line broadening (**Figure 2B**). Relying on this approach, we
238 observed a similarly strong chemical shift change also when adding Pr^{3+} to a glyphosate solution
239 containing liposomes (**Figure 2C**). While the non-permeable Pr^{3+} interacted with glyphosate
240 outside of the liposomes influencing the chemical shift, the shift agent could not enter the
241 liposomes as demonstrated by the observation that inside the glyphosate the chemical shift was
242 left unchanged. As a consequence, two distinct peaks appeared in the spectrum, and the glyphosate
243 peak outside the liposomes was well-resolved from the peak inside. This indicated that the

244 exchange was slow on the NMR timescale; that is, the ratio $k_{tr}/\Delta\delta_H$ is smaller than one ($k_{tr}/\Delta\delta_H < 1$),
245 where k_{tr} is the apparent rate constant of exchange and $\Delta\delta_H$ is the chemical shift difference in ^{1}H-
246 NMR.[47] The glyphosate exchange across the liposome bilayer was fast enough, however, to lead
247 to considerable line broadening, $\Delta\upsilon$, of the inside peak. The line broadening $\Delta\upsilon$ depends on the
248 apparent rate constant of exchange k_{tr} according to equation (2)[37] and ranged from $\Delta\upsilon$ = 2.6 Hz at
249 neutral pH to $\Delta\upsilon$ = 40.8 Hz at pH 4.

250 The glyphosate peaks inside the liposomes were fitted to determine the peak width prior to (υ_0)

$$\Delta\upsilon = \frac{k_{tr}}{\pi} \quad (2)$$

251 and after addition of $PrCl_3$ (υ_{ex}). The resultant line broadening $\Delta\upsilon = \upsilon_{ex} - \upsilon_0$ (**Figure 2C**) was used
252 to calculate k_{tr} for each liposome preparation.

253 **Glyphosate permeation of lipid bilayers depends strongly on pH.** Because k_{tr} strongly
254 depends on the surface area and on the size of the liposomes, k_{tr} is not suitable to compare the
255 chemical exchange of different liposome preparations and at different pH values. Therefore, Males
256 *et al*. derived the apparent permeation coefficient P_{app} [m·s^{-1}] by including the inner liposome
257 volume and the volume-to-surface ratio according to equation (3),[37] where d_{lip} is the diameter of
258 the respective liposome and δ is the membrane thickness (4 nm); note that this membrane thickness
259 δ should not be confused with the chemical shift δ_H (or δ_P) in the NMR spectrum or the isotope
260 value $\delta^{13}C$. Our NMR approach is not subject to aqueous boundary layer effects (i.e., the
261 permeation coefficient so determined is that of the lipid bilayer alone). The NMR experiments
262 measured a dynamic exchange process under equilibrium conditions. The k_{tr} does, however,
263 include a contribution from glyphosate diffusing a short distance through water to arrive at the
264 lipid bilayer surface. We therefore refer to our rate constant of exchange as an apparent value, and
265 the permeation coefficient derived from it as an apparent permeation coefficient, P_{app}:

$$P_{app} = \frac{k_{tr} \times (d_{lip} - 2\delta)}{6} = \frac{\Delta v \times \pi \times (d_{lip} - 2\delta)}{6} \quad (3)$$

The permeation coefficient describes how rapidly glyphosate permeates a hypothetical two-dimensional POPC membrane sheet and was much higher than expected (**Figure 3A**). At circumneutral pH the apparent permeation coefficient of glyphosate (double negatively charged, molecular weight MW = 167 g·mol^{-1}) P_{app}(pH 7.0) = 3.7 (± 0.3) × 10^{-7} m·s^{-1} was considerably higher than the one of maleate[46] (double negatively charged, MW = 114 g·mol^{-1}) and in the same range as the permeation coefficient of the polar, neutral serotonin species (MW = 176 g·mol^{-1}).[58] With decreasing pH, the permeation rate increased, with an apparent permeation coefficient of P_{app}(pH 4.1) = 4.2 (± 0.1) × 10^{-6} m·s^{-1} at pH 4.1. The pH-dependence correlated linearly with the average degree of ionization and thus the average charge of glyphosate (**Figure 3B**). The net charge of –2 (one positive and three negative charges) of glyphosate at neutral pH slowed passive membrane permeation. Protonation of the phosphate group at pH 4.1 reduced the net charge of glyphosate to –1 and, consequently, accelerated membrane permeation. This also indicates that the effect of Pr^{3+} on the measured permeation coefficient is negligible. If the change towards positive liposome surface potential due to Pr^{3+} addition (*vide supra*) facilitated permeation due to attraction of the strongly negatively charged glyphosate, the doublely negatively charged glyphosate species would permeate faster. However, the opposite is the case. Furthermore, that two distinct glyphosate peaks appear in the NMR spectrum (*vide supra*) demonstrates that Pr^{3+} does not enter the liposomes together with glyphosate which could lead to changed permeation characteristics. Therefore, we hypothesize that the zwitterionic structure of glyphosate facilitates glyphosate permeation, whereas the increased negative charge at neutral pH slowed passive permeation of glyphosate.

287 **Membrane permeation can lead to considerable glyphosate uptake into bacterial cells.** The
288 entry of non-polar pollutants into bacterial cells by passive permeation of the cell envelope is well
289 recognized,[30, 59] and charged, polar molecules like glyphosate are commonly assumed to be taken
290 up almost exclusively by active transport or porin-assisted permeation.[60, 61] Contrary to this
291 expectation, our observations in a liposome model system that lacked transporters or porins gave
292 membrane permeation coefficients of glyphosate in the same range as those of non-charged
293 molecules (see above).[58] This observation suggests that passive membrane permeation of
294 glyphosate mono- and dianions may provide sufficient influx into bacterial cells for it to serve as
295 phosphorus source. Because the diffusion through water of glyphosate is fast compared with the
296 diffusion through the lipid membrane,[62, 63], the membrane as significant barrier influences how
297 fast the molar amount of substrate outside the bacteria n_{out} is reduced via passive membrane
298 permeation at the rate $(dn_{out}/dt)_{permeation}$. This process is driven by the concentration gradient across
299 the membrane and is defined by the linear exchange term in equation (4) as proposed by Males *et*
300 *al.*.[64]

$$(\frac{dn_{out}}{dt})_{permeation} = -(k_{tr}K_{lip-w}[S_{out}]) + (k_{tr}K_{lip-w}[S_{in}]) \quad (4)$$

301 Here, $K_{lip\text{-}w}$ is the membrane lipid-water partitioning coefficient, $[S_{out}]$ and $[S_{in}]$ are the
302 glyphosate concentrations outside and inside the bacterial cell, whereas $K_{lip\text{-}w}[S_{out}]$ and $K_{lip\text{-}w}[S_{in}]$
303 are the concentrations within the lipid membrane (outside and inside), respectively. With the
304 definition of the diffusion coefficient across the membrane (lipid bilayer) D_{lip} (5), the apparent rate
305 constant of exchange k_{tr} can be calculated for a single bacterial cell by equation (6)

$$D_{lip} = \frac{P_{app} \times \delta}{K_{lip-w}} \quad (5)$$

$$k_{tr} = \frac{D_{lip} \times A_{cell}}{\delta} = \frac{P_{app} \times A_{cell}}{K_{lip-w}} \quad (6)$$

306 where $A_{cell} \approx 3$ μm^2 is the estimated surface area of one bacterial cell and δ is the membrane
307 thickness (one 4 nm membrane in Gram-positive and two 4 nm thick membranes which equals
308 8 nm in total in Gram-negative bacteria). Together with equation (7), a term is obtained for the
309 concentration gradient-dependent glyphosate influx of a single bacterial cell:

$$\left(\frac{dn_{out}}{dt}\right)_{cell-permeation} = -(P_{app}A_{cell}[S_{out}]) + (P_{app}A_{cell}[S_{in}]) \quad (7)$$

310 The glyphosate influx is at its maximum $(dn_{out}/dt)_{cell\text{-}permeation\text{-}max}$ when the concentration gradient
311 is large ($[S_{in}] = 0$). We compared this maximum permeation rate with the glyphosate degradation
312 rate of *Achromobacter sp.* MPS 12A described by Sviridov *et al.*.[22] The glyphosate degradation
313 rate of a single *Achromobacter sp.* MPS 12A cell $(dn/dt)_{deg\text{-}cell} = -1.4 \times 10^{-21}$ mol·s^{-1}·cell^{-1} at a
314 concentration of 3 mM[22] was estimated by correlating the number of cells with the optical density
315 OD_{600} and the bulk glyphosate degradation rate. While this correlation strongly depends on the
316 strain and the growth conditions, the previously reported value of 8×10^8 cells·mL^{-1}·OD_{600}^{-1}
317 provides a good first estimate.[65, 66] The comparison showed that the calculated maximum
318 membrane permeation rate at pH 7 $(dn_{out}/dt)_{cell\text{-}perm\text{-}max} = -1.9 \times 10^{-18}$ mol·s^{-1}·cell^{-1} was two orders
319 of magnitude higher than the degradation rate. As a consequence, even though glyphosate has a
320 net charge of –2 at pH 7, its passive membrane permeation is predicted to be fast enough to provide
321 enough influx for bacterial biodegradation and to serve as phosphorus source. This hypothesis
322 clearly warrants further testing. If true, it should be possible to confirm it (a) by the observation of
323 similarly rapid biodegradation per cell in a different strain and (b) by applying compound-specific
324 isotope fractionation as a diagnostic tool to observe the absence of mass transfer limitations
325 directly. If permeation is indeed faster than enzymatic conversion, glyphosate molecules inside

326 and outside the cell are expected to be in rapid equilibrium. Thus, glyphosate molecules enriched
327 in heavy isotopes due to the enzymatic reaction in the cytosol will get out of the cell into the bulk
328 solution. This would lead to the isotope effect of the enzyme reaction being observable outside the
329 cell, resulting in strong isotope fractionation during biodegradation. A new bacterium was,
330 therefore, isolated from soil, and isotope fractionation was measured during glyphosate
331 degradation.

332 **Isolation and glyphosate degradation activity of *Orchrobactrum sp.* FrEM.** Repeated
333 subculturing of an inoculum from soil samples in a medium containing 3 mM glyphosate as sole
334 phosphorus source resulted in the isolation of a bacterial strain with glyphosate-degrading activity.
335 Glyphosate was only used as phosphorus source. Shushkova *et al.* faced difficulties when isolating
336 a strain with glyphosate as carbon and phosphorus source.[67] The bacteria were rod-shaped as
337 observed by light microscopy (**SI Figure S2**). Sequence alignment (BLAST) of the 16S rRNA
338 showed a 99% homology with *Ochrobactrum anthropic, O. rhizosphaerae*, *O. pituitosum,* and *O.*
339 *intermedium*, which all belong to the family of Brucellaceae of Alphaproteobacteria, and 70%
340 homology with *Ochrobactrum haematophilum.* The strain was termed *Ochrobactrum sp.* FrEM
341 (**SI Figure S3**). The fastest glyphosate degradation by *O. sp.* FrEM occurred after 4.5 days when
342 the cell density was high ($OD_{600} \approx 0.8$). Within 12 h, the glyphosate concentration decreased from
343 104 mM to 55 mM equaling a maximum glyphosate degradation rate $(dn/dt)_{deg\text{-}cell} = -1.7 \times 10^{-}$
344 ^{21} mol·s^{-1}·cell^{-1} (**Figure 4A**) which was as high as that of *Achromobacter sp.* MPS 12A (see
345 above).[22] Furthermore, just as for *Achromobacter sp.* MPS 12A, the calculated maximum
346 membrane permeation rate at pH 7 $(dn_{out}/dt)_{cell\text{-}perm\text{-}max} = -7.5 \times 10^{-20}$ mol·s^{-1}·cell^{-1} at a
347 concentration of 0.12 mM was larger than the degradation rate indicating that passive permeation

348 of the cell envelope is likely not rate limiting for glyphosate biodegradation. We subsequently
349 aimed to verify this hypothesis by compound-specific isotope fractionation analysis.

350 **Carbon isotope fractionation revealed rapid glyphosate mass transfer across the cell wall.**
351 Glyphosate biodegradation by *O. sp.* FrEM (**Figure 4A**) was accompanied by significant carbon
352 isotope fractionation. Carbon isotope values $\delta^{13}C$ of glyphosate increased from –28 (± 0.5) ‰ in
353 the beginning to –19 (± 0.5) ‰ after 90% glyphosate conversion reflecting an enrichment of ^{13}C
354 over ^{12}C. The corresponding enrichment factor $\varepsilon^{13}C$ = –4.5 (± 0.5) ‰ was determined according
355 to the Rayleigh equation (**Figure 5**, and equation (1)). The primary apparent kinetic isotope effect
356 AKIE, a measure for the isotope effect at the reactive position, allows the direct comparison of
357 isotope effects of different reactions and reactants and was calculated according to equation (8)[68]

$$AKIE_{carbon} = \frac{1}{\frac{n}{x}\varepsilon^{13}C+1} \quad (8)$$

358 where n denotes the total number of carbon atoms and x the number of carbon atoms at the
359 reactive position. With $n = 3$ and $x = 1$, the primary apparent kinetic isotope effect for glyphosate
360 degradation (via breaking a single bond between carbon and phosphorous) was
361 $AKIE_{carbon} = 1.014 \pm 0.003$, which is in the range of chemical reactions that involve breaking a
362 single bond to a carbon atom.[68, 69]

363 This suggests that any additional rate determining steps like active transport[33] or slow passive
364 membrane permeation[31] masked the enzymatic isotope fractionation only to a small extent, if at
365 all. As a consequence, we conclude that, indeed, glyphosate exchanged rapidly across the cell
366 envelope consistent with our hypothesis that passive permeation across the cell envelope may be
367 an important, and until now underestimated, driver to facilitate biodegradation of glyphosate or
368 other charged pollutants (C, N, P sources). Future research should not only address the role of pH

369 in the permeation of whole cells during biodegradation but also elucidate the possible role of
370 transporters or porins (e.g., by studying isotope fractionation during glyphosate degradation in cell
371 free extracts of *O. sp.* FrEM or with liposomes containing the degrading enzyme).

372 **Possibility of mass transfer limitations at low concentrations in the environment.** While
373 passive membrane permeation has previously been associated with only non-polar molecules, our
374 results suggest that also charged species like glyphosate can enter the bacterial cell not only
375 assisted by proteins, e.g. by active transporters[70, 71] or facilitated diffusion via porins,[29, 72] but also
376 by passive permeation of the cell membrane more rapidly than commonly thought. This can
377 facilitate glyphosate biodegradation and lead to rapid turnover at high concentrations in water and
378 soil.[10] A different situation must be considered, however, if the concentration gradient across the
379 cell envelope is shallower, that is, when the outside concentration is lower. While the degradation-
380 associated isotope fractionation was determined at high concentrations (> 25 μM) the
381 concentration in soil and ground- and surface waters is much lower (< 2 μM, < 15 nM, and
382 < 0.5 μM respectively).[18, 73] We recently demonstrated that mass transfer across the cell membrane
383 becomes rate-limiting for atrazine biodegradation at trace concentrations.[25] Similarly, at a
384 glyphosate concentration of 1 μM, the calculated maximum membrane permeation rate is reduced
385 to only $(dn_{out}/dt)_{cell\text{-}perm\text{-}max} = -6.5 \times 10^{-22}$ mol·s^{-1}·cell^{-1}, which is lower than the respective
386 degradation rate per cell. At these concentrations, acceleration of cell wall transfer of glyphosate
387 with high affinity active transporters may become necessary to boost biodegradation. Interestingly,
388 Pipke *et al.* described such an active glyphosate transporter with an uptake rate of $(dn_{out}/dt)_{cell\text{-}}$
389 $_{transport} = -1.8 \times 10^{-21}$ mol·s^{-1}·cell^{-1} which is just in the range of observed glyphosate degradation
390 rates.[74] However, its affinity constant $K_M = 0.125$ mM for glyphosate uptake is rather high,
391 resulting in low transporter activity at trace concentrations. This increased mass transfer limitation

392 at trace concentrations may cause biodegradation to stall and might explain the frequent detection
393 of glyphosate in the environment.[17]
394
395 ASSOCIATED CONTENT

396 A list of chemicals, media composition, and strain isolation, figures of the glyphosate spectra,
397 Micrograph of *Ochrobactrum sp* FrEM, phylogenetic tree, LC-IRMS chromatogram, and a table
398 summarizing spectra collection parameters (PDF). This information is available free of charge via
399 the Internet at http://pubs.acs.org.

400 AUTHOR INFORMATION

401 **Corresponding Author**

402 *ME: Chair of Analytical Chemistry and Water Chemistry, Technical University of Munich,
403 Marchioninistrasse 17, 81377 Munich, Germany, m.elsner@tum.de, +49 89 2180-78232

404 * JAP: Departments of Soil Science and Civil & Environmental Chemistry, University of
405 Wisconsin, Madison, WI 53706, USA, joelpedersen@wisc.edu, +1 608 263 4971

406 **Author Contributions**

407 The manuscript was written through contributions of all authors. All authors have given approval
408 to the final version of the manuscript.

409 **Funding Sources**

410 This work was funded by an ERC consolidator grant (“MicroDegrade”, grant no. 616861).

411 ACKNOWLEDGMENT

This work was funded by an ERC consolidator grant ("MicroDegrade", grant no. 616861) awarded by the European Research Council to M.E. The NMR instrumentation was supported by a generous gift from Paul J. and Margaret M. Bender to the Magnetic Resonance Facility in the Chemistry Department of the University of Wisconsin-Madison. J.A.P. gratefully acknowledges the support of the William A. Rothermel Bascom Professorship.

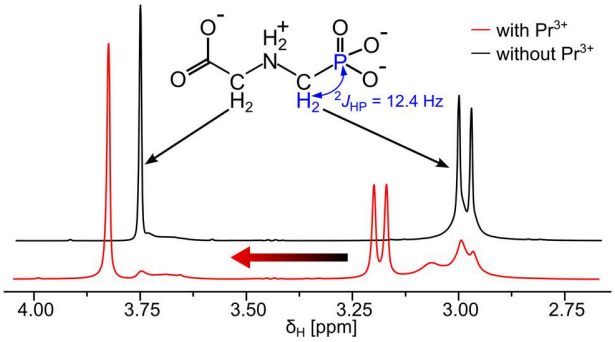

Figure 1. $^2J_{HP}$ coupling prevents direct measurement of glyphosate permeation of liposomes with standard ^{1}H-spectra. Glyphosate showed one singlet at 3.74 ppm and one doublet at 2.99 ppm in the ^{1}H NMR spectrum with solvent suppression (black line). Strong $^2J_{HP}$ coupling led to formation of a doublet centered at 2.99 ppm. Upon Pr^{3+} addition to the liposome suspension, the spectrum changed (red line). The glyphosate peaks outside the liposomes were shifted downfield (doublet at 3.2 ppm and singlet at 3.79 ppm) and the peaks inside the liposomes broadened due to chemical exchange. As a consequence, the individual doublet peaks overlapped, almost coalescing into a singlet and rendering peak shape analysis impossible. Both spectra in this figure were collected at pH 7.5.

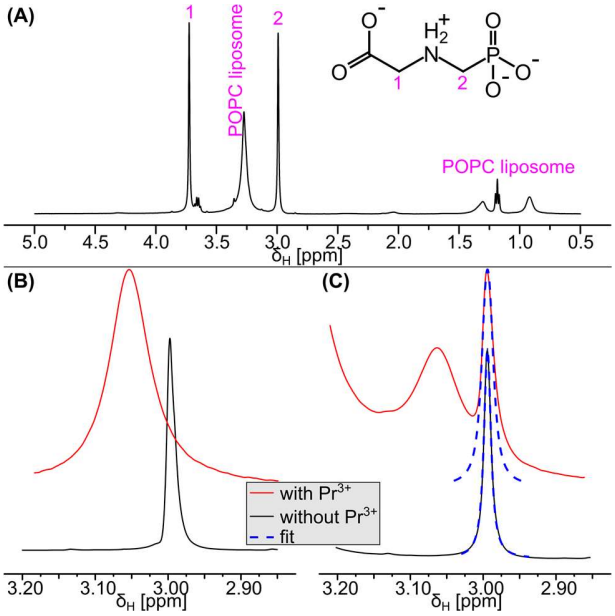

Figure 2. Peak shape broadening due to exchange can be quantified by fitting the peaks in $^{1}H\{^{31}P\}$ NMR spectra. (A) Clear separation of the glyphosate signals from the signals of the POPC liposomes in the $^{1}H\{^{31}P\}$ NMR spectrum (black line) enabling reliable peak shape analysis. **(B)** Spectral region showing glyphosate protons attached to carbon 2 with (red line) and without Pr^{3+} (black line) in the absence of liposomes. The line broadening upon Pr^{3+} addition was caused by the interaction with the paramagnetic Pr^{3+}. Even though the signal without Pr^{3+} slightly overlapped with the broad glyphosate signal in the presence of Pr^{3+}, both peaks were well resolved. **(C)** The glyphosate peaks inside and outside the liposomes remained well resolved when POPC liposomes were present. Fitting the peak shape (blue dashed lines) prior (black line) and after (red line) the addition of $PrCl_3$ yielded peak widths and, thus, allowed the line broadening to be quantified. The broadening of the glyphosate peak inside the liposomes (2.99 ppm) was caused by chemical exchange of glyphosate between the inside and the outside of the liposomes, because the non-permeable Pr^{3+} was not able to interact with glyphosate inside the liposomes. All spectra in this figure were collected at pH 7.5.

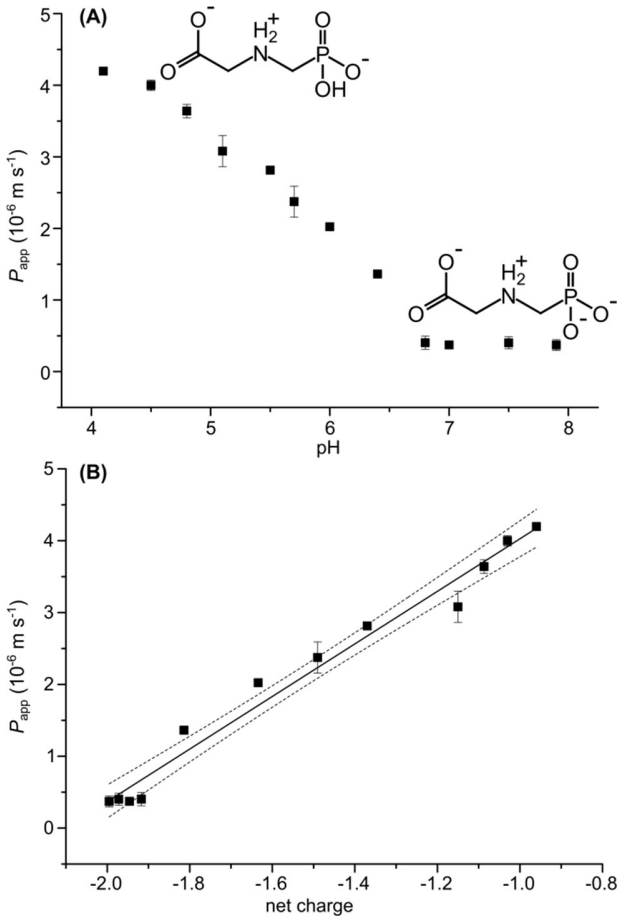

Figure 3. The pH-dependence of the permeation coefficient P_{app} (black squares) correlated with the net charge of glyphosate. (A) P_{app} depended strongly on the pH of the liposome solution. The permeation at neutral pH (P_{app}(pH 7.0) = 3.7 (± 0.3) × 10^{-7} m·s^{-1}) was one order of magnitude lower than at slightly acidic pH (P_{app}(pH 4.1) = 4.2 (± 0.1) × 10^{-6} m·s^{-1}). (B) Permeation correlated with the ionization of glyphosate which can be explained by two different permeation coefficients of the two different glyphosate species (two negative and one negative charge at the phosphate group, respectively). Both panels show the mean and the error bars depicting the standard deviation.

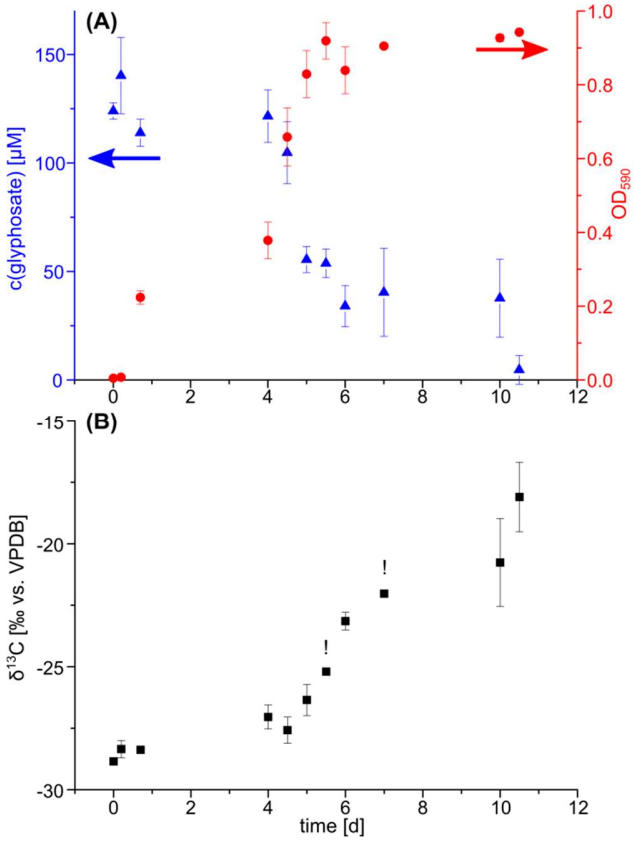

Figure 4. Glyphosate biodegradation was accompanied by growth and strong isotope fractionation. (A) Glyphosate degradation by *Ochrobactrum sp.* FrEM. Consumption of glyphosate (blue triangles) as source of phosphorous led to bacterial growth (red circles). **(B)** During this biodegradation, $^{13}C/^{12}C$ ratios of glyphosate increased, as indicated by less negative $\delta^{13}C$ values. All graphs show the mean and the error bars indicating the range of two biological replicates. The exclamation marks (!) above two isotope data points indicate that a reliable isotope value could be measured for only one biological replicate at the respective time points. Isotope values were measured in technical triplicates for each sample and are associated with an analytical uncertainty of ± 0.3 ‰.

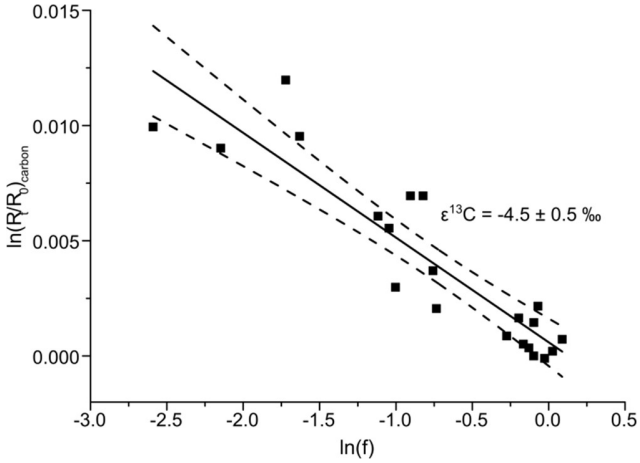

Figure 5. Pronounced isotope fractionation indicated rapid glyphosate exchange across the bacterial cell envelope. The carbon isotope fractionation factor ($\varepsilon^{13}C = -4.5$ ($\pm$ 0.5) ‰) was determined according to the Rayleigh equation (equation (1)). The corresponding $AKIE_{carbon}$ = 1.014 ± 0.003 (see equation (8)) was in the range of typical carbon isotope effects. This indicated that the enzymatic isotope fractionation was not masked by mass transfer limitations and that exchange of glyphosate across the cell envelope was comparatively rapid during bacterial degradation by *Ochrobactrum sp.* FrEM.

REFERENCES

1. Franz, J. E.; Mao, M. K.; Sikorski, J. A., *Glyphosate: a unique global herbicide*. American Chemical Society: 1997.
2. Dill, G. M.; Sammons, R. D.; Feng, P. C. C.; Kohn, F.; Kretzmer, K.; Mehrsheikh, A.; Bleeke, M.; Honegger, J. L.; Farmer, D.; Wright, D.; Haupfear, E. A., Glyphosate: Discovery, Development, Applications, and Properties. In *Glyphosate Resistance in Crops and Weeds*, John Wiley & Sons, Inc.: 2010; pp 1-33.
3. Duke, S. O.; Powles, S. B., Glyphosate: a once-in-a-century herbicide. *Pest Management Science* **2008,** *64*, (4), 319-325.
4. Dill, G. M., Glyphosate-resistant crops: history, status and future. *Pest Management Science* **2005,** *61*, (3), 219-224.
5. Bøhn, T.; Cuhra, M.; Traavik, T.; Sanden, M.; Fagan, J.; Primicerio, R., Compositional differences in soybeans on the market: Glyphosate accumulates in Roundup Ready GM soybeans. *Food Chemistry* **2014,** *153*, 207-215.
6. Woodburn, A. T., Glyphosate: production, pricing and use worldwide. *Pest Management Science* **2000,** *56*, (4), 309-312.
7. USGS Estimated Annual Agricultural Pesticide Use. https://water.usgs.gov/nawqa/pnsp/usage/maps/show_map.php?year=2015&map=GLYPHOSATE&hilo=H&disp=Glyphosate (05.04.2018),
8. Helander, M.; Saloniemi, I.; Saikkonen, K., Glyphosate in northern ecosystems. *Trends in Plant Science* **2012,** *17*, (10), 569-574.
9. Relyea, R. A., THE LETHAL IMPACT OF ROUNDUP ON AQUATIC AND TERRESTRIAL AMPHIBIANS. *Ecological Applications* **2005,** *15*, (4), 1118-1124.
10. Giesy, J. P.; Dobson, S.; Solomon, K. R., Ecotoxicological Risk Assessment for Roundup® Herbicide. In *Reviews of Environmental Contamination and Toxicology: Continuation of Residue Reviews*, Ware, G. W., Ed. Springer New York: New York, NY, 2000; pp 35-120.
11. Sullivan, T. P.; Sullivan, D. S., Vegetation management and ecosystem disturbance: impact of glyphosate herbicide on plant and animal diversity in terrestrial systems. *Environmental Reviews* **2003,** *11*, (1), 37-59.
12. Mamy, L.; Gabrielle, B.; Barriuso, E., Comparative environmental impacts of glyphosate and conventional herbicides when used with glyphosate-tolerant and non-tolerant crops. *Environmental Pollution* **2010,** *158*, (10), 3172-3178.
13. Firbank, L. G.; Forcella, F., Genetically Modified Crops and Farmland Biodiversity. *Science* **2000,** *289*, (5484), 1481-1482.
14. WHO, IARC Monographs: evaluation of five organophosphate insecticides and herbicides. *WHO* **2015,** *112*.
15. Chang, E. T.; Delzell, E., Systematic review and meta-analysis of glyphosate exposure and risk of lymphohematopoietic cancers. *Journal of Environmental Science and Health, Part B* **2016,** *51*, (6), 402-434.
16. Andreotti, G.; Koutros, S.; Hofmann, J. N.; Sandler, D. P.; Lubin, J. H.; Lynch, C. F.; Lerro, C. C.; De Roos, A. J.; Parks, C. G.; Alavanja, M. C.; Silverman, D. T.; Beane Freeman, L. E., Glyphosate Use and Cancer Incidence in the Agricultural Health Study. *JNCI: Journal of the National Cancer Institute* **2017**, djx233, https://doi.org/10.1093/jnci/djx233.

17. Mamy, L.; Barriuso, E.; Gabrielle, B., Environmental fate of herbicides trifluralin, metazachlor, metamitron and sulcotrione compared with that of glyphosate, a substitute broad spectrum herbicide for different glyphosate-resistant crops. *Pest management science* **2005,** *61*, (9), 905-916.
18. Battaglin, W. A.; Meyer, M. T.; Kuivila, K. M.; Dietze, J. E., Glyphosate and Its Degradation Product AMPA Occur Frequently and Widely in U.S. Soils, Surface Water, Groundwater, and Precipitation. *J. Am. Water Resour. Assoc.* **2014,** *50*, (2), 275-290.
19. Horth, H.; Blackmore, K., Survey of glyphosate and AMPA in groundwaters and surface waters in Europe. *Report by WRc plc, Swindon, Swindon, Wiltshire, United Kingdom. No.: UC8073* **2009,** *2*.
20. Ermakova, I.; Kiseleva, N.; Shushkova, T.; Zharikov, M.; Zharikov, G.; Leontievsky, A., Bioremediation of glyphosate-contaminated soils. *Applied Microbiology and Biotechnology* **2010,** *88*, (2), 585-594.
21. Pipke, R.; Amrhein, N., Degradation of the Phosphonate Herbicide Glyphosate by Arthrobacter atrocyaneus ATCC 13752. *Applied and Environmental Microbiology* **1988,** *54*, (5), 1293-1296.
22. Sviridov, A. V.; Shushkova, T. V.; Zelenkova, N. F.; Vinokurova, N. G.; Morgunov, I. G.; Ermakova, I. T.; Leontievsky, A. A., Distribution of glyphosate and methylphosphonate catabolism systems in soil bacteria Ochrobactrum anthropi and Achromobacter sp. *Applied Microbiology and Biotechnology* **2012,** *93*, (2), 787-96.
23. Borggaard, O. K.; Gimsing, A. L., Fate of glyphosate in soil and the possibility of leaching to ground and surface waters: a review. *Pest Management Science* **2008,** *64*, (4), 441-456.
24. Bosma, T. N. P.; Middeldorp, P. J. M.; Schraa, G.; Zehnder, A. J. B., Mass Transfer Limitation of Biotransformation: Quantifying Bioavailability. *Environ. Sci. Technol.* **1997,** *31*, (1), 248-252.
25. Ehrl, B. N.; Kundu, K.; Gharasoo, M.; Marozava, S.; Elsner, M., Rate limiting mass transfer in micropollutant degradation revealed by isotope fractionation. *Environ. Sci. Technol.* **submitted, attached as supporting information for review only**.
26. Sprankle, P.; Meggitt, W.; Penner, D., Adsorption, mobility, and microbial degradation of glyphosate in the soil. *Weed Science* **1975,** *23*, 229-234.
27. Button, D. K., Kinetics of nutrient-limited transport and microbial growth. *Microbiol. Rev.* **1985**, (49), 270-297.
28. Ferenci, T.; Robert, K. P., Bacterial Physiology, Regulation and Mutational Adaptation in a Chemostat Environment. In *Advances in Microbial Physiology*, Academic Press: 2008; Vol. Volume 53, pp 169-315.
29. Delcour, A. H., Outer Membrane Permeability and Antibiotic Resistance. *Biochimica et biophysica acta* **2009,** *1794*, (5), 808-816.
30. Parales, R. E.; Ditty, J. L., Substrate Transport. In *Handbook of Hydrocarbon and Lipid Microbiology*, Timmis, K. N., Ed. Springer Berlin Heidelberg: Berlin, Heidelberg, 2010; pp 1545-1553.
31. Ehrl, B. N.; Gharasoo, M.; Elsner, M., Isotope Fractionation Pinpoints Membrane Permeability as a Barrier to Atrazine Biodegradation in Gram-negative Polaromonas sp. Nea-C. *Environ. Sci. Technol.* **2018,** *52*, (7), 4137-4144.
32. Wick, L. M.; Quadroni, M.; Egli, T., Short- and long-term changes in proteome composition and kinetic properties in a culture of Escherichia coli during transition from glucose-

557 excess to glucose-limited growth conditions in continuous culture and vice versa. *Environmental*
558 *Microbiology* **2001,** *3*, (9), 588-599.
559 33. Qiu, S.; Gözdereliler, E.; Weyrauch, P.; Lopez, E. C. M.; Kohler, H.-P. E.; Sørensen, S.
560 R.; Meckenstock, R. U.; Elsner, M., Small 13C/12C Fractionation Contrasts with Large
561 Enantiomer Fractionation in Aerobic Biodegradation of Phenoxy Acids. *Environ. Sci. Technol.*
562 **2014,** *48*, (10), 5501-5511.
563 34. Beate I. Escher, L. S., Chemical Speciation of Organics and of Metals at Biological
564 Interphases. In *Physicochemical Kinetics and Transport at Biointerfaces*, Hermann P. Van
565 Leeuwen, W. K., Ed. Wiley: 2004; Vol. 9, pp 205-269.
566 35. Wohnsland, F.; Faller, B., High-Throughput Permeability pH Profile and High-Throughput
567 Alkane/Water log P with Artificial Membranes. *Journal of Medicinal Chemistry* **2001,** *44*, (6),
568 923-930.
569 36. Passeleu-Le Bourdonnec, C.; Carrupt, P.-A.; Scherrmann, J. M.; Martel, S., Methodologies
570 to Assess Drug Permeation Through the Blood–Brain Barrier for Pharmaceutical Research.
571 *Pharmaceutical Research* **2013,** *30*, (11), 2729-2756.
572 37. Males, R. G.; Herring, F. G., A 1H-NMR study of the permeation of glycolic acid through
573 phospholipid membranes. *Biochimica et Biophysica Acta (BBA) - Biomembranes* **1999,** *1416*, (1–
574 2), 333-338.
575 38. Naderkhani, E.; Vasskog, T.; Flaten, G. E., Biomimetic PVPA in vitro model for estimation
576 of the intestinal drug permeability using fasted and fed state simulated intestinal fluids. *European*
577 *Journal of Pharmaceutical Sciences* **2015,** *73*, 64-71.
578 39. Lande, M. B.; Donovan, J. M.; Zeidel, M. L., The relationship between membrane fluidity
579 and permeabilities to water, solutes, ammonia, and protons. *The Journal of General Physiology*
580 **1995,** *106*, (1), 67-84.
581 40. Dietrich, C.; Bagatolli, L. A.; Volovyk, Z. N.; Thompson, N. L.; Levi, M.; Jacobson, K.;
582 Gratton, E., Lipid Rafts Reconstituted in Model Membranes. *Biophysical Journal* **2001,** *80*, (3),
583 1417-1428.
584 41. Xiang, T.-X.; Anderson, B. D., Development of a combined NMR paramagnetic ion-
585 induced line-broadening/dynamic light scattering method for permeability measurements across
586 lipid bilayer membranes. *Journal of Pharmaceutical Sciences* **1995,** *84*, (11), 1308-1315.
587 42. Russell, N. J.; Fukunaga, N., A comparison of thermal adaptation of membrane lipids in
588 psychrophilic and thermophilic bacteria. *FEMS Microbiology Letters* **1990,** *75*, (2-3), 171-182.
589 43. Sharon, V.; Dina, P.; Ehud, P.; H., P. A.; Itzhak, F., Coexistence of Domains with Distinct
590 Order and Polarity in Fluid Bacterial Membranes¶. *Photochemistry and Photobiology* **2002,** *76*,
591 (1), 1-11.
592 44. Epand, R. M.; Epand, R. F., Lipid domains in bacterial membranes and the action of
593 antimicrobial agents. *Biochimica et Biophysica Acta (BBA) - Biomembranes* **2009,** *1788*, (1), 289-
594 294.
595 45. Vollmer, W.; Blanot, D.; De Pedro, M. A., Peptidoglycan structure and architecture. *FEMS*
596 *Microbiology Reviews* **2008,** *32*, (2), 149-167.
597 46. Prestegard, J. H.; Cramer, J. A.; Viscio, D. B., Nuclear magnetic resonance determinations
598 of permeation coefficients for maleic acid in phospholipid vesicles. *Biophysical Journal* **1979,** *26*,
599 (3), 575-584.
600 47. Millet, O.; Loria, J. P.; Kroenke, C. D.; Pons, M.; Palmer, A. G., The Static Magnetic Field
601 Dependence of Chemical Exchange Linebroadening Defines the NMR Chemical Shift Time Scale.
602 *J. Am. Chem. Soc.* **2000,** *122*, (12), 2867-2877.

48. Melander, L.; Saunders, W. H., *Reaction rates of isotopic molecules*. John Wiley: New York, 1980; p 331.
49. Hoefs, J., Theoretical and Experimental Principles. In *Stable isotope geochemistry*, 3rd ed.; Wyllie, P. J., Ed. Springer-Verlag: Chicago, 1987; pp 1-25.
50. Schmidt, H. L., Fundamentals and systematics of the non-statistical distributions of isotopes in natural compounds. *Naturwissenschaften* **2003,** *90*, (12), 537-552.
51. Thullner, M.; Kampara, M.; Richnow, H. H.; Harms, H.; Wick, L. Y., Impact of Bioavailability Restrictions on Microbially Induced Stable Isotope Fractionation. 1. Theoretical Calculation. *Environ. Sci. Technol.* **2008,** *42*, (17), 6544-6551.
52. Kampara, M.; Thullner, M.; Richnow, H. H.; Harms, H.; Wick, L. Y., Impact of Bioavailability Restrictions on Microbially Induced Stable Isotope Fractionation. 2. Experimental Evidence. *Environ. Sci. Technol.* **2008,** *42*, (17), 6552-6558.
53. Thullner, M.; Fischer, A.; Richnow, H. H.; Wick, L. Y., Influence of mass transfer on stable isotope fractionation. *Applied Microbiology and Biotechnology* **2013,** *97*, (2), 441-452.
54. MacDonald, R. C.; MacDonald, R. I.; Menco, B. P. M.; Takeshita, K.; Subbarao, N. K.; Hu, L.-r., Small-volume extrusion apparatus for preparation of large, unilamellar vesicles. *Biochimica et Biophysica Acta (BBA) - Biomembranes* **1991,** *1061*, (2), 297-303.
55. Hope, M. J.; Bally, M. B.; Webb, G.; Cullis, P. R., Production of large unilamellar vesicles by a rapid extrusion procedure. Characterization of size distribution, trapped volume and ability to maintain a membrane potential. *Biochimica et Biophysica Acta (BBA) - Biomembranes* **1985,** *812*, (1), 55-65.
56. Kujawinski, D. M.; Wolbert, J. B.; Zhang, L.; Jochmann, M. A.; Widory, D.; Baran, N.; Schmidt, T. C., Carbon isotope ratio measurements of glyphosate and AMPA by liquid chromatography coupled to isotope ratio mass spectrometry. *Analytical and Bioanalytical Chemistry* **2013,** *405*, (9), 2869-2878.
57. Moncelli, M. R.; Becucci, L.; Guidelli, R., The intrinsic pKa values for phosphatidylcholine, phosphatidylethanolamine, and phosphatidylserine in monolayers deposited on mercury electrodes. *Biophysical Journal* **1994,** *66*, (6), 1969-1980.
58. Viscio, D. B.; Prestegard, J. H., NMR studies of 5-hydroxytryptamine transport through large unilamellar vesicle membranes. *Proceedings of the National Academy of Sciences of the United States of America* **1981,** *78*, (3), 1638-1642.
59. Endo, S.; Escher, B. I.; Goss, K.-U., Capacities of Membrane Lipids to Accumulate Neutral Organic Chemicals. *Environ. Sci. Technol.* **2011,** *45*, (14), 5912-5921.
60. Kallimanis, A.; Frillingos, S.; Drainas, C.; Koukkou, A. I., Taxonomic identification, phenanthrene uptake activity, and membrane lipid alterations of the PAH degrading Arthrobacter sp. strain Sphe3. *Applied Microbiology and Biotechnology* **2007,** *76*, (3), 709-717.
61. Kell, D. B.; Dobson, P. D.; Oliver, S. G., Pharmaceutical drug transport: the issues and the implications that it is essentially carrier-mediated only. *Drug Discovery Today* **2011,** *16*, (15–16), 704-714.
62. Culbertson, C. T.; Jacobson, S. C.; Michael Ramsey, J., Diffusion coefficient measurements in microfluidic devices. *Talanta* **2002,** *56*, (2), 365-373.
63. Worch, E., A new equation for the calculation of diffusion coefficients for dissolved substances. In *[Water]*, Fachgruppe Wasserchemie In Der Gesellschaft Deutscher, C., Ed. 1993; Vol. 81, pp 289-297.
64. Males, R. G.; Phillips, P. S.; Herring, F. G., Equations describing passive transport through vesicular membranes. *Biophysical Chemistry* **1998,** *70*, (1), 65-74.

649 65. Volkmer, B.; Heinemann, M., Condition-Dependent Cell Volume and Concentration of
650 Escherichia coli to Facilitate Data Conversion for Systems Biology Modeling. *PLOS ONE* **2011,**
651 *6*, (7), e23126.
652 66. Kopinke, F.-D.; Georgi, A.; Roland, U., Isotope fractionation in phase-transfer processes
653 under thermodynamic and kinetic control – Implications for diffusive fractionation in aqueous
654 solution. *Science of The Total Environment* **2018,** *610-611*, (Supplement C), 495-502.
655 67. Shushkova, T. V.; Ermakova, I. T.; Sviridov, A. V.; Leontievsky, A. A., Biodegradation
656 of glyphosate by soil bacteria: Optimization of cultivation and the method for active biomass
657 storage. *Microbiology* **2012,** *81*, (1), 44-50.
658 68. Elsner, M.; Zwank, L.; Hunkeler, D.; Schwarzenbach, R. P., A new concept linking
659 observable stable isotope fractionation to transformation pathways of organic pollutants. *Environ.*
660 *Sci. Technol.* **2005,** *39*, (18), 6896-6916.
661 69. Mancini, S. A.; Hirschorn, S. K.; Elsner, M.; Lacrampe-Couloume, G.; Sleep, B. E.;
662 Edwards, E. A.; SherwoodLollar, B., Effects of Trace Element Concentration on Enzyme
663 Controlled Stable Isotope Fractionation during Aerobic Biodegradation of Toluene. *Environ. Sci.*
664 *Technol.* **2006,** *40*, (24), 7675-7681.
665 70. Muller, R. H.; Hoffmann, D., Uptake kinetics of 2,4-dichlorophenoxyacetate by Delftia
666 acidovorans MC1 and derivative strains: Complex characteristics in response to pH and growth
667 substrate. *Bioscience Biotechnology and Biochemistry* **2006,** *70*, (7), 1642-1654.
668 71. Nichols, N. N.; Harwood, C. S., PcaK, a high-affinity permease for the aromatic
669 compounds 4-hydroxybenzoate and protocatechuate from Pseudomonas putida. *Journal of*
670 *Bacteriology* **1997,** *179*, (16), 5056-61.
671 72. Button, D. K.; Robertson, B.; Gustafson, E.; Zhao, X. M., Experimental and theoretical
672 bases of specific affinity, a cytoarchitecture-based formulation of nutrient collection proposed to
673 supercede the Michaels-Menten paradigm of microbial kinetics. *Applied and Environmental*
674 *Microbiology* **2004,** *70*, (9), 5511-5521.
675 73. Sanchis, J.; Kantiani, L.; Llorca, M.; Rubio, F.; Ginebreda, A.; Fraile, J.; Garrido, T.; Farre,
676 M., Determination of glyphosate in groundwater samples using an ultrasensitive immunoassay and
677 confirmation by on-line solid-phase extraction followed by liquid chromatography coupled to
678 tandem mass spectrometry. *Analytical and Bioanalytical Chemistry* **2012,** *402*, (7), 2335-2345.
679 74. Pipke, R.; Schulz, A.; Amrhein, N., Uptake of Glyphosate by an Arthrobacter sp. *Applied*
680 *and Environmental Microbiology* **1987,** *53*, (5), 974-978.

681